FIRST SIMULTANEOUS DETERMINATION OF SIZE, REFRACTIVE INDEX, LIGHT SCATTERING DEPOLARIZATION AND FLUORESCENCE OF PHYTOPLANKTON CELLS BY LASER SCANNING FLOW CYTOMETRY

Luca Fiorani[1], Roberta Fantoni[1], Antonia Lai[1], Antonio Palucci[1], Konstantin A. Semyanov[2], Maria Sighicelli[1], Valeria Spizzichino[1] and Peter A. Tarasov[2]

1. Laser Applications Section, ENEA, 45 Fermi Street, 00044 Frascati, Italy; fiorani(at)frascati.enea.it
2. Institute of Chemical Kinetics and Combustion, SB RAS, 3 Institutskaya Street, 630090 Novosibirsk, Russia

ABSTRACT

A new laser flow cytometer, based on a laser source of polarized light irradiating microscopic particles, has been developed. The unpolarized and linearly polarized scattered light, as well as the side emitted light in different spectral bands, are measured, allowing the simultaneous and real-time determination of size, refractive index, light scattering depolarization and fluorescence of each particle. Tests with aqueous samples of polystyrene spheres, fluorescent or non fluorescent, and phytoplankton cells demonstrate that the system is able to retrieve size and refractive index and that the light scattering depolarization and fluorescence measurements allows the sorting of particles otherwise indistinguishable.

Keynotes: light scattering, fluorescence, polarization, laser flow cytometry.

INTRODUCTION

The simultaneous determination of size and refractive index of microscopic particles by laser systems is based on Mie theory that describes the light scattering by dielectric spheres (1). In general, instruments based on this technique are named laser particle counters (2) and laser flow cytometers (3), if the particles are suspended in air and water, respectively. The great interest for the fast sorting of microscopic particles in liquid suspensions (marine phytoplankton, blood cells, etc.) favoured the broad diffusion of commercial systems based on laser flow cytometry (LFC).

In LFC, the particle flow and the laser beam are orthogonal. When a particle crosses the beam, the radiation is scattered with an angular distribution that depends on size, shape and refractive index. In general, in commercial systems, only the forward scattering (FSC) and the side scattering (SSC) are measured, without retrieving size and refractive index. Often, the particle fluorescence is detected in some spectral bands. The forward scattering is associated with the particle size (4), while side scattering is dominated by refractive effects (5). Although these are simplifications, this approach allows the fast sorting of cells both in oceanographic (6) and clinical (7) fields, especially if the cells are marked with monoclonal antibodies conjugated to fluorescent dyes.

Typically, LFC allows to acquire five parameters simultaneously: forward scattering, side scattering and fluorescence in 3 spectral bands (e.g. FACScan from Becton, Dickinson and Company). The counting rate can exceed 10 thousand particles per second. Among the advantages of LFC we recall the easy sample preparation, the absence of chemical treatment and the possibility of *in situ* measurements.

Recently, the CLASS laser flow cytometer (CLASS is the acronym of *Citometro LAser in fluSSo*, i.e. the Italian translation of *laser flow cytometer*) has been patented (8). CLASS has been realised for the characterization of phytoplankton cells at the laboratories of Frascati of the Laser Application Section (LAS) of the Italian Agency for New Technologies, Energy and the Environment (ENEA), in collaboration with the Institute of Chemical Kinetics and Combustion (ICKC) of the Siberian Branch of the Russian Academy of Science (SB RAS).

Taking into account that:

- phytoplankton cells can be discriminated not only by size and refractive index, but also *via* deviation from spherical shape and pigmentation,
- deviation from spherical shape and pigmentation can be observed thanks to light scattering depolarization and fluorescence emission, respectively,

a research line has been developed to reach the objective of the first simultaneous determination of size, refractive index, light scattering depolarization and fluorescence of microscopic particles.

To this respect, LAS and ICKC carried out complementary research for more than a decade: LAS developed local and remote sensors based on laser-induced fluorescence (LIF) for bio-optical measurements of natural waters (9), and ICKC demonstrated the first example of laser scanning flow cytometry (LSFC) (10), able to retrieve size and refractive index. Both research lines resulted in prototype patents (11,12). Moreover, one of the authors used polarizing optics in the laser radar which he realized during his PhD thesis (13).

By combining LIF, LSFC and polarizing optics the laser flow cytometer CLASS has been developed, resulting in an innovative system able to simultaneously measure size, refractive index, light scattering depolarization and fluorescence of microscopic particles in liquid suspension.

INSTRUMENTS AND METHODS

A picture of the instrument is shown in Figure 1, the optical scheme is provided in Figure 2. The optical elements are described in Table 1. Although CLASS represents the first application of LSFC to phytoplankton cells (14), the more innovative part of the system consists of the measurement of light scattering depolarization of microscopic particles. In order to carry it out, it has been necessary to use a diode laser with a high polarization ratio (100:1). Moreover, that source is characterised by large power and short wavelength, allowing the system to have good sensitivity and to detect sub-micrometric particles (up to about half of the wavelength). Potentially, it is possible to increase the polarization ratio inserting a Glan-Taylor polarizer (Thorlabs GT10, clear aperture diameter 10 mm, extinction ratio 100,000:1) in the beam. The linearly polarized beam, after having been bent by three mirrors in order to make the system compact, gets across a quarter-wave plate, going out circularly polarized. Later, after having been focused by a lens and having got across a mirror with hole, the beam coaxially falls on particles in liquid suspension that flows across the capillary (diameter: 254 μm) of a cuvette. In the interaction region (length less than 5 mm) the beam has a small cross section with a diameter around 30 μm FWHM so that the radiant energy is high. The light scattered by the particle is reflected by the spherical mirror forming the bottom of the cuvette towards the mirror with a hole. The radiation reflected by this mirror, after having been bent by another mirror in order to reduce the size of the system, is divided in two parts by a non-polarizing beam splitter. The transmitted part is detected by the photomultiplier PM_1, after having traversed a polarizer, the reflected one is detected as it is by the photomultiplier PM_2. Beam splitter, polarizer and photomultipliers are mounted on an aluminium block. That mechanical mount filters the background radiation and transmits only the light coming from the mirror with hole. A variable diaphragm performs the spatial filtering of the input beam.

For each position of the particle along the capillary only the light coming from a well defined scattering polar angle, that is the radiation collimated by the spherical mirror, is detected. Consequently, by retrieving the position from the acquisition time of the signal, thanks to the measurement of the particle velocity and its transit time in a known point, it is possible to determine the scattering intensity as a function of the polar angle (indicatrix) in a wide interval (typically between 5° and 100°). Size and refractive index of the particles can then be retrieved from the indicatrix by an inversion method (15) of the Mie theory. The transit time of the particle in a known point is measured, as shown below, by observing the side scattering. The particle velocity is a previously calibrated function of the pressures in the hydrodynamic circuit, selected by the operator.

If the particles were spherical, the signals I_1 and I_2, at the output of the photomultipliers PM_1 and PM_2, respectively, would be the same (except for a constant factor, linked to the different efficiency

of the respective detection channels, which can be made equal to 1 by adjusting the gain of the photomultipliers). If, conversely, the particles are not spherical, the light scattering depolarization

$$\delta I = I_1 - I_2 \tag{1}$$

is not zero. Consequently, the light scattering depolarization measurement allows to discriminate spherical particles: this is particularly useful to sort phytoplankton cells.

In order to demonstrate it, we calculate I_1 and I_2 using the Mueller formalism (16). The radiation that incides on the particle has left-hand circular polarization. The corresponding Stokes vector is:

$$V_i = \begin{bmatrix} 1 \\ 0 \\ 0 \\ -1 \end{bmatrix}. \tag{2}$$

The Mueller matrices relative to particle scattering, beam splitter and polarizer are, respectively:

$$S = \begin{bmatrix} s_{11} & s_{12} & s_{13} & s_{14} \\ s_{21} & s_{22} & s_{23} & s_{24} \\ s_{31} & s_{32} & s_{33} & s_{34} \\ s_{41} & s_{42} & s_{43} & s_{44} \end{bmatrix}, \tag{3}$$

where each element of S is a function of the polar (θ) and azimuthal (φ) scattering angles,

$$B = \begin{bmatrix} 1/2 & 0 & 0 & 0 \\ 0 & 1/2 & 0 & 0 \\ 0 & 0 & 1/2 & 0 \\ 0 & 0 & 0 & 1/2 \end{bmatrix} \tag{4}$$

and

$$P = \begin{bmatrix} 1 & 1 & 0 & 0 \\ 1 & 1 & 0 & 0 \\ 0 & 0 & 0 & 0 \\ 0 & 0 & 0 & 0 \end{bmatrix}. \tag{5}$$

The Stokes vector of the photomultiplier is:

$$V_{PM} = \begin{bmatrix} 1 & 0 & 0 & 0 \end{bmatrix}. \tag{6}$$

Since the azimuthal angles in the laboratory system and in the particle system do not coincide, the laboratory-particle rotation matrix has to be applied:

$$M_{\varphi} = \begin{bmatrix} 1 & 0 & 0 & 0 \\ 0 & \cos(2\varphi) & \sin(2\varphi) & 0 \\ 0 & -\sin(2\varphi) & \cos(2\varphi) & 0 \\ 0 & 0 & 0 & 1 \end{bmatrix} \tag{7}$$

and the particle-laboratory rotation matrix:

$$M_{-\varphi} = \begin{bmatrix} 1 & 0 & 0 & 0 \\ 0 & \cos(2\varphi) & -\sin(2\varphi) & 0 \\ 0 & \sin(2\varphi) & \cos(2\varphi) & 0 \\ 0 & 0 & 0 & 1 \end{bmatrix}. \tag{8}$$

Moreover, it is necessary to integrate over φ between 0 and 2π, because the reflectance of the spherical mirror of the cuvette is independent of the azimuthal angle. Eventually, we can write:

$$I_1 = k_1 \int_0^{2\pi} V_{PM}\ P\ B\ M_{-\varphi}\ S\ M_{\varphi}\ V_i\ d\varphi\,, \tag{9}$$

$$I_2 = k_2 \int_0^{2\pi} V_{PM}\ B\ M_{-\varphi}\ S\ M_{\varphi}\ V_i\ d\varphi\,, \tag{10}$$

where k_1 and k_2 are constant factors, linked to the efficiencies of the respective detection channels. Developing the calculus, we obtain:

$$I_1 = k_1 \int_0^{2\pi} \left[s_{11} - s_{14} + (s_{21} - s_{24})\cos(2\varphi) - (s_{31} - s_{34})\sin(2\varphi)\right] d\varphi\,, \tag{11}$$

$$I_2 = k_2 \int_0^{2\pi} (s_{11} - s_{14})\, d\varphi\,. \tag{12}$$

For spherical particles:

$$I_1 = k_1 \int_0^{2\pi} s_{11}\, d\varphi\,, \tag{13}$$

$$I_2 = k_2 \int_0^{2\pi} s_{11}\, d\varphi\,. \tag{14}$$

After having introduced spherical particles in the experimental system and having tuned the gain of photomultipliers PM_1 and PM_2 so that:

$$k_1 = k_2 = k\,, \tag{15}$$

it follows:

a) in general:

$$I_1 = k \int_0^{2\pi} \left[s_{11} - s_{14} + (s_{21} - s_{24})\cos(2\varphi) - (s_{31} - s_{34})\sin(2\varphi)\right] d\varphi\,, \tag{16}$$

$$I_2 = k \int_0^{2\pi} (s_{11} - s_{14})\, d\varphi\,, \tag{17}$$

$$\delta I = k \int_0^{2\pi} \left[(s_{21} - s_{24})\cos(2\varphi) - (s_{31} - s_{34})\sin(2\varphi)\right] d\varphi\,, \tag{18}$$

b) for spherical particles:

$$I_1 = k \int_0^{2\pi} s_{11}\, d\varphi\,, \tag{19}$$

$$I_2 = k \int_0^{2\pi} s_{11}\, d\varphi\,, \tag{20}$$

$$\delta I = 0\,. \tag{21}$$

The system also observes the side radiation by a microscope objective. The light is split into three spectral zones by two dichroic mirrors. The reflection of the first dichroic mirror sends the side scattering to the photomultiplier PM_5 that measures the transit time of the particle in a known point and provides the trigger to the experiment. The photomultiplier is mounted on an aluminium block

allowing only the light coming from the particle to pass. A variable diaphragm and an interference filter perform the spatial and spectral filtering, respectively, of the input beam. The second dichroic mirror:

- reflects the green radiation towards the photomultiplier PM_4 that measures the fluorescence of the particle around 530 nm, after spectral filtering carried out by an interference filter,
- transmits the red radiation to the photomultiplier PM_3 that measures the fluorescence of the particle around 680 nm, after the spectral filtering carried out by an interference filter.

The photomultipliers and the interference filters are mounted on an aluminium block allowing only the light coming from the particle to pass. A variable diaphragm performs the spatial filtering of the input beam.

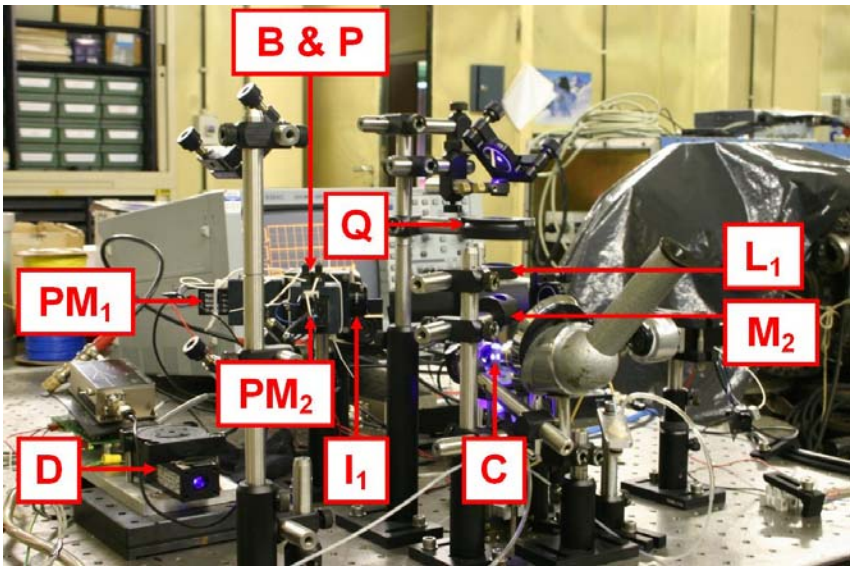

Figure 1: Picture of the system. The main elements are indicated with the naming convention following in Table 1.

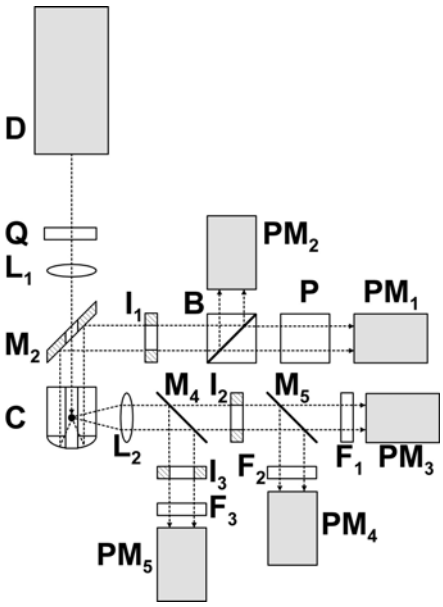

Figure 2: Optical scheme of the system. The elements are described in Table 1. The three bending mirrors M_1 (inserted between D and Q) and the bending mirror M_3 inserted between M_2 and I_1) are not influential and have not been indicated.

Table 1. Optical elements of the system. λ: wavelength, ∅: diameter, AOI: angle of incidence, R: reflectance, AR: anti reflection, f: focal length, h: height, NA: numerical aperture, T: transmittance, CA: clear aperture, BW: bandwidth.

Element	Description	Characteristics	Producer/Model
D	Diode laser	λ: 405 nm, power: 50 mW, polarization ratio: 100:1	µLS/Lepton IV
M_1	Broadband dielectric mirror	∅: 25.4 mm, AOI: 45°, R>97% (400 – 750 nm)	Micos
Q	Zero order quarter-wave plate	λ: 405 nm, ∅: 12.7 mm, AR coating at 405 nm	Micos
L_1	Plano-convex lens	f: 60 mm, R<3% (350 – 650 nm)	Thorlabs/LA1134-A
M_2	Broadband dielectric mirror with hole	∅: 25.4 mm, hole ∅: 1 mm, R>97% (400 – 750 nm)	Micos
C	Cuvette with spherical mirror	∅: 5 mm, h: 5 mm	ICKC
M_3	Broadband dielectric mirror	∅: 25.4 mm, AOI: 0°–45°, R>98% (400–800 nm)	Thorlabs/BB1-E02
I_1	Variable iris diaphragm	∅: 2 mm	Thorlabs/D12S
B	Non polarizing beam splitter cube	Side: 10 mm, T and R>40% (400–600 nm)	Thorlabs/BS010
P	Glan-Thompson polarizer	CA ∅: 10 mm, extinction ratio 100,000:1	Thorlabs/GTH10M
PM_1	Photomultiplier module	λ: 300 – 650 nm (peak: 420 nm), sensitivity: 4.3×10^4 A/W. Connected to the amplifier Femto HCA-10M-100K-C	Hamamatsu/H6780
PM_2	Photomultiplier module	λ: 185 – 650 nm (peak: 420 nm), sensitivity: 4.3×10^4 A/W. Connected to the amplifier Analog Modules 352-1-B-1M	Hamamatsu/H6780-03
L_2	Microscope objective	Magnification: 50×, NA: 0.55	Zeiss/LD EC Epiplan-Neofluar
M_4	Dichroic mirror	∅: 25.4 mm, AOI: 45°, R>90% (405 nm) T>70% (>435 nm)	Laser Components /630DRLP
I_2	Variable iris diaphragm	∅: 4 mm	Thorlabs/D12S
M_5	Dichroic mirror	∅: 25.4 mm, AOI: 45°, R>90% (460 – 620 nm) T>70% (>660 nm)	Laser Components /435DRLP
F_1	Interference filter	∅: 25.4 mm, T: 74% (680 nm), BW: 11 nm	Laser Components /680DF10
PM_3	Photomultiplier module	λ: 300 – 900 nm (peak: 630 nm), sensitivity: 3.9×10^4 A/W. Connected to the amplifier Femto HCA-1M-1M-C	Hamamatsu/H6780-20
F_2	Interference filter	∅: 25.4 mm, T: 64% (530 nm), BW: 6 nm	Omega Optical/530BP5
PM_4	Photomultiplier module	Λ: 185 – 850 nm (peak: 400 nm), sensitivity: 3.0×10^4 A/W. Connected to the amplifier Femto HCA-1M-1M-C	Hamamatsu/H6780-04
I_3	Variable iris diaphragm	∅: 1 mm	Thorlabs/D12S
F_3	Interference filter	∅: 25.4 mm, T: 51% (402 nm), BW: 5 nm	Omega Optical/403BP5
PM_5	Photomultiplier module	λ: 185 – 750 nm (peak: 420 nm), sensitivity: 5.2×10^5 A/W. Connected to the amplifier Analog Modules 352-1-B-1M	Hamamatsu/H7710-11

The signals detected by the photomultipliers are amplified by the transimpedance amplifiers indicated in Table 1, digitised by the analog-to-digital converter ADLINK DAQ-2010 (4 channels, 14 bits, 2 MS/s) and stored and analysed in an industrial personal computer. The interface of the acquisition and analysis programme (FastSFC) is shown in Figure 3. Once the sample has been inserted (typically some thousands of particles), the system analyses it in a few minutes providing size, refractive index, light scattering depolarization and fluorescence of each particle.

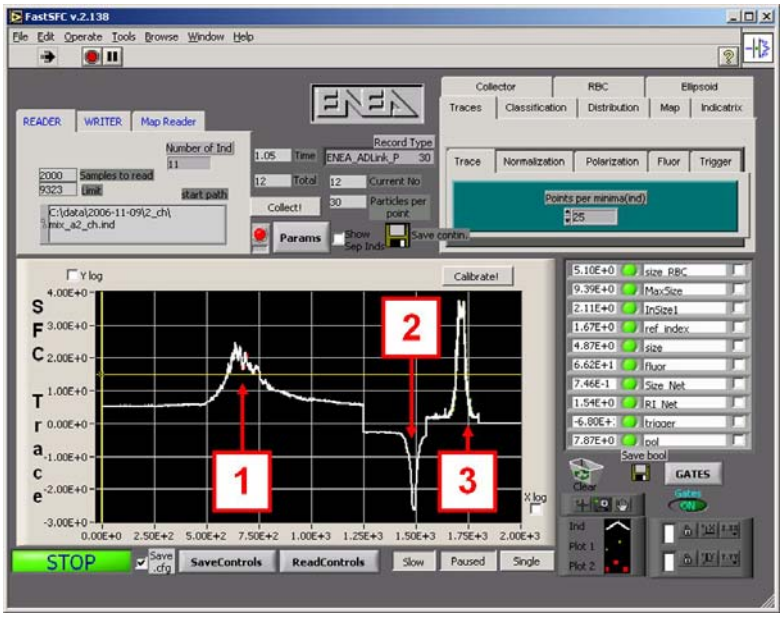

Figure 3: Interface of the acquisition and analysis programme. The traces 1, 2 and 3 represent signals corresponding to the indicatrix, trigger and fluorescence (the second has been inverted for ease of vision).

RESULTS AND DISCUSSION

We will illustrate the operation of CLASS describing the measurement of a sample of *Chlamydomonas reinhardtii*, an eukaryote single celled green alga, about 10 µm long, that moves using two flagella, about 10 µm long (Figure 4). This cell offers an ideal test for the system having elliptic shape and containing chlorophyll-a that imply non-zero light scattering depolarization and fluorescence around 680 nm, respectively. The results of the test, illustrated in Figure 5 and Table 2, were obtained with a sample of *Chlamydomonas reinhardtii* (hereafter referred as "*chlamydomonas*") mixed with fluorescent and non-fluorescent polystyrene spheres, having 6 µm diameter, (indicated as "6 µm F" and "6 µm NF", respectively).

Figure 4: Optical microscopic image of Chlamydomonas reinhardtii obtained at the laboratories of LAS shortly before the measurement with CLASS.

First of all, one observes that the instrument measures correctly the size and the refractive index of the spheres. In fact, the expected values: 6.0 µm and 1.61 – 1.62 (14), respectively, are compatible with the retrieved values (15): 6.07±0.27 µm and 1.629±0.022, respectively (obtained by averaging the results of 6 µm F and 6 µm NF), corresponding to relative errors of 1% in both cases. Moreover, as we expected, all the spheres have zero light scattering depolarization and the fluorescence is different from zero only with the 6 µm F spheres.

As far as the particle sorting is concerned, due to the large natural variability in size of the cells (observed at the microscope), the corresponding histogram is rather wide and it is impossible to distinguish them from the spheres. Also for the refractive index an analogous argument holds: although the values for cells and spheres are significantly different, it exists a non-negligible overlap in the histograms: a cell can be mistaken as a sphere and vice versa. The situation becomes better if fluorescence is observed: the non-fluorescent spheres are completely resolved. Unfortunately, there still can be confusion between fluorescent spheres and cells. Eventually, whenever the light scattering depolarization is taken into account, it is impossible to mistake cells and spheres.

These results are even more evident in the two-dimensional and three-dimensional scatter plots of Figure 6 and 7, respectively, and demonstrate how useful is the light scattering depolarization measurement for the accurate sorting of microscopic particles: without it, it would have been impossible to fully distinguish cells and spheres.

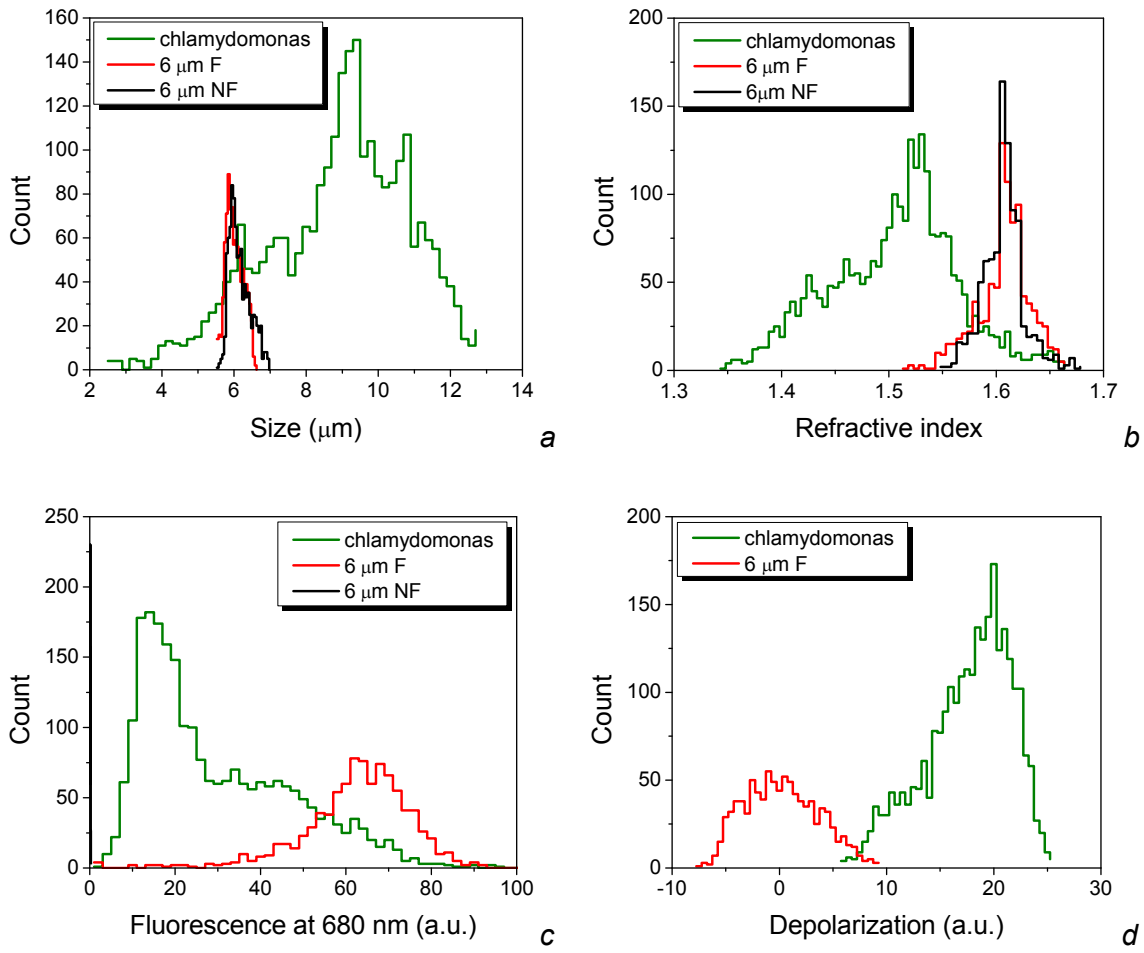

Figure 5: Histograms of: a) size, b) refractive index, c) fluorescence and d) light scattering depolarization obtained analysing a sample of Chlamydomonas reinhardtii mixed with fluorescent and non-fluorescent polystyrene spheres having 6 µm diameter.

Table 2: Determinations of size, refractive index, light scattering depolarization and fluorescence obtained analysing a sample of Chlamydomonas reinhardtii mixed with fluorescent and non-fluorescent polystyrene spheres having 6 µm diameter. N: number of particles, M: mean, SD: standard deviation.

Particle	N	Size (µm)		Refractive index		Depolarization (a.u.)		Fluorescence (a.u.)	
		M	SD	M	SD	M	SD	M	SD
Chlamydomonas	2627	8.79	1.97	1.526	0.059	17.4	4.0	26	19
6 µm F	924	6.00	0.24	1.629	0.025	0.0	3.5	61	13
6 µm NF	909	6.13	0.29	1.629	0.019	0.1	3.5	0	0

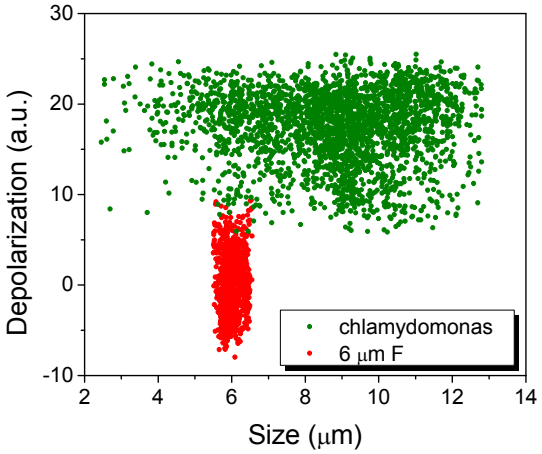

Figure 6: Two-dimensional scatter plot (size and light scattering depolarization) obtained analysing a sample of Chlamydomonas reinhardtii mixed with fluorescent polystyrene spheres having 6 µm diameter.

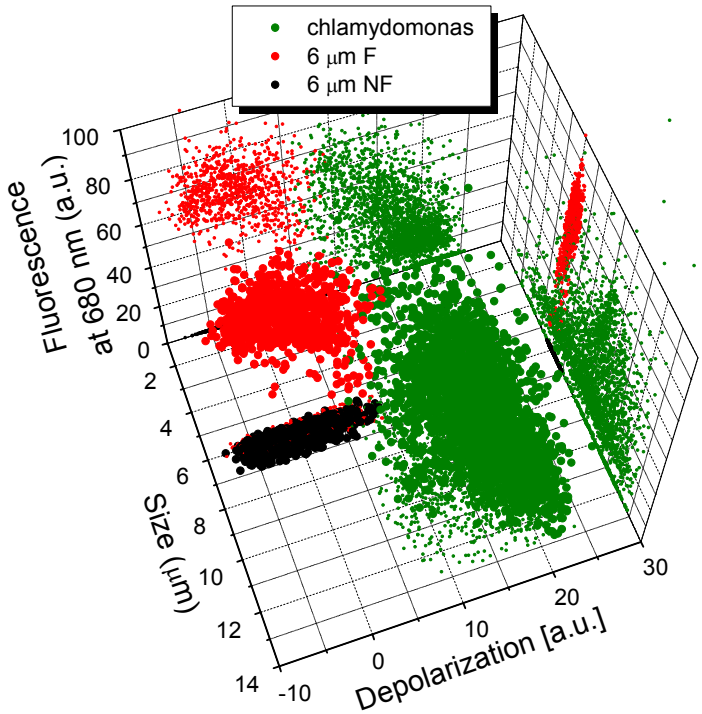

Figure 7: Three-dimensional scatter plot (size, light scattering depolarization and fluorescence) obtained analysing a sample of Chlamydomonas reinhardtii mixed with fluorescent and non-fluorescent polystyrene spheres having 6 µm diameter (the smaller points are the projections on the planes).

In order to give an example of the potentiality of the fluorescence observation in two spectral bands, a sample has been measured which was prepared by mixing green fluorescent and non-fluorescent polystyrene spheres having 2 µm diameter (indicated as “2 µm F” and “2 µm NF”, respectively), with red fluorescent and non-fluorescent polystyrene spheres having 6 µm diameter (indicated as “6 µm F” and “6 µm NF”, respectively). The three-dimensional scatter plot (Figure 8) demonstrates that CLASS resolves the four types of particles in well distinct clouds of points.

Although those results are very promising, it has to be recognised that the full potentiality of fluorescent spectroscopy has not been exploited by the observation of two fluorescence bands. A substantial improvement of the system would be the recording of the full fluorescence spectrum, allowing one to detect different phytoplankton pigments. That perspective is really exciting and two different solutions to achieve it are under study (implementing a compact spectrometer or dispersive optics).

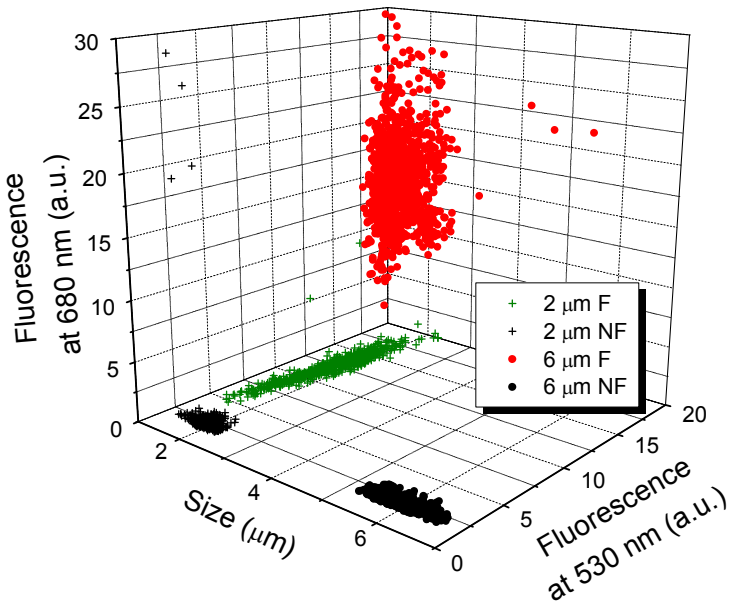

Figure 8: Three-dimensional scatter plot (size, fluorescence at 530 nm and fluorescence at 680 nm) obtained analysing a sample prepared by mixing green fluorescent and non-fluorescent polystyrene spheres with 2 µm diameter, and red fluorescent and non-fluorescent polystyrene spheres with 6 µm diameter.

CONCLUSIONS

A new laser flow cytometer (CLASS), has been developed. Its more relevant feature is the introduction of a polarized source and the detection of unpolarized and linearly polarized scattered light. Thanks to that innovation, simultaneous determinations of size, refractive index, light scattering depolarization and fluorescence of microscopic particles have been carried out. To our knowledge, they represent the first example of those results by laser flow cytometry.

The tests conducted on polystyrene spheres show that some thousands of particles can be analysed in few minutes and indicate that the accuracy of CLASS in the retrieval of size and refractive index can exceed 1% in that particular case.

CLASS has been applied to the experimental characterization of phytoplankton cells. Those researches confirm the role of fluorescence measurements and, more important, demonstrate the role of light scattering depolarization measurements in the sorting of particles otherwise indistinguishable by size and refractive index determinations.

ACKNOWLEDGEMENTS

The authors are deeply grateful to P. Aristipini for technical drawings, R. Giovagnoli for mechanical parts, F. Barnaba and V. M. Nekrasov for system tests and P. Albertano for chlamydomonas samples. This work has been supported by the Italian Ministry of University and Research (MUR) in the frame of the project Microsystems for Hostile Environments (MIAO).

REFERENCES

1 Tsang L, J A Kong & K-H Ding, 2000. Scattering of Electromagnetic Waves: Theories and Applications (John Wiley & Sons, New York) 426 pp.

2 Provder T & J Texter, eds., 2004. Particle Sizing and Characterization (American Chemical Society, Washington) 292 pp.

3 Shapiro H M, 2003. Practical Flow Cytometry (John Wiley & Sons, New York) 681 pp.

4 Burger D E, J H Jett & P F Mullaney, 1982. Extraction of morphological features from biological models and cells by Fourier analysis of static light scatter measurements. Cytometry, 2, 327-336

5 Salzman G C, P F Mullaney & B J Price, 1979. Light-scattering approaches to cell characterization. In: Flow Cytometry and Sorting, edited by M R Melamed, T Lindmo & M Mendelsohn (John Wiley & Sons, New York) 108-124

6 Dubelaar G B J & R R Jonker, 2000. Flow cytometry as a tool for the study of phytoplankton. Scientia Marina, 64: 135-156

7 O'Leary T J, 1998. Flow cytometry in diagnostic cytology. Diagnostic Cytopathology 18: 41-46

8 Fiorani L, A Palucci, V Maltsev & K Semyanov, 2007. Citometro laser in flusso per la misura simultanea di taglia, indice di rifrazione, asfericità e fluorescenza di particelle microscopiche in sospensioni liquide o gassose (Italian Patent Number: RM2007A000371)

9 Fiorani L & A Palucci, 2006. Local and remote laser sensing of bio-optical parameters in natural waters. Journal of Computational Technologies, 11: 39-45

10 Maltsev V P, 2000. Scanning flow cytometry for individual particle analysis, Review of Scientific Instruments, 71: 243-255

11 Aristipini P, L Fiorani, I Menicucci & A Palucci, 2005. Spettrofluorimetro laser portatile per l'analisi in situ dei liquidi non opachi (Italian Patent Number: RM2005A000269)

12 Maltsev V P & A V Chernyshev, 1997. Method and device for determination of parameters of individual microparticles (United States Patent Number: 5650847)

13 Fiorani L, 1996. Une première mesure lidar combinée d'ozone et de vent, à partir d'une instrumentation et d'une méthodologie coup par coup (Swiss Federal Institute of Technology, Lausanne) 180 pp.

14 Barnaba F, L Fiorani, A Palucci & P Tarasov, 2006. First characterization of marine particles by laser scanning flow cytometry. Journal of Quantitative Spectroscopy and Radiative Transfer 102: 11-17.

15 Semyanov K A, P A Tarasov, A E Zharinov, A V Chernyshev, A G Hoekstra & V P Maltsev, 2004. Single-particle sizing from light scattering by spectral decomposition. Applied Optics, 43: 5110-5115

16 Guenther R, 1990. Modern Optics (John Wiley & Sons, New York) 696 pp.